A Novel Capacitor Voltage Balancing Strategy for Modular Multilevel Converters.

Matías Urrutia
U. Técnica Federico Santa María (UTFSM), Santiago, Chile
matias.urrutia@alumnos.usm.cl

Andrés Mora, Alejandro Angulo and Pablo Lezana
UTFSM,Valparaíso, Chile
andres.mora@usm.cl

Roberto Cárdenas
Universidad de Chile
Santiago, Chile
rcd@ieee.org

Matías Diaz
U. Santiago de Chile
Santiago, Chile
matias.diazd@usach.cl

***Abstract*—This paper presents a simple and innovative Capacitor Voltage Balancing (CVB) strategy for Modular Multilevel Converters (MMC) based on full H-bridge cell topologies. The method computes specific modulation indexes for each cell using the explicit solution of an underlying optimal control problem. Based on the structure of its analytical solution, the proposed CVB scheme is integrated to a Phase-Shifted PWM scheme with an easy implementation. Experimental results obtained from a nine-cell single-phase converter demonstrate an improved performance of the proposed method, especially under transient operating conditions.**

***Index Terms*—Modular Multilevel Converters, H-bridges, floating capacitor, voltage balancing, phase-shifted PWM.**

I. Introduction

Multilevel converters are a widely accepted technology with successful insertion in high power and medium voltage industrial applications. High-quality output voltages, the possibility to reach higher voltage levels without increasing semiconductors rated capability, and the modular structure are their most attractive features [1, 2]. Among their different topologies, MMCs have acquired special interest due to their completely modular design, its scalability without increasing the components rate, the possibility of a transformerless configuration, and its fault-tolerant operation capability. [2–5].

MMCs fundamental component is the power cell, which is based on power semiconductors and a floating capacitor. The set of n cells and an inductor connected in series constitute an arm (or branch), whose interconnections define specific topologies of MMCs family [2, 3]. For instance, the modular multilevel matrix converter (M3C) is composed of two three-phase AC ports interconnected through nine arms (or branches) as shown Fig. 1(a). Applications of this kind of converter in high-power electrical drives and wind energy conversion systems have been reported [6–8].

The operation and control of the MMCs is more complex than that of conventional converters due to the floating capacitors. For the proper operation of these converters, it is essential to keep the voltage of all capacitors within a feasible tolerance range. In this regard, several control strategies have been proposed in the literature, where the following aims are frequently sought [7, 9–11]: to control the total energy supplied to the converter, to balance the energy between the all arms and, to locally balance the energy of the cells belonging the same cluster. The latter is known as capacitor voltage balancing strategy (or local balancing control). The strategies introduced in previous work can be grouped as those which use additional reference signals in the modulation scheme [11, 12], and those that modifies the cell's switching patterns according to the capacitor's voltages [9, 13, 14]. Both approaches require information of the current flow direction in the arm and, they are closely linked to the modulation scheme used to generate the converter output voltage.

In the literature, two conventional multicarrier pulsewidth modulation (PWM) strategies are typically used to modulate the MMC: the phase-shifted (PS-PWM) and the level-shifted (LS-PWM) [15–17]. Regarding the PS-PWM strategy, in [7, 11, 12], a proportional controller for each cell is proposed to locally balance the capacitor voltages. In this method, the present capacitor voltage is compared to its desired value, and the resulting error is multiplied by the sign of the arm current to obtain a compensation signal. This signal is then added to the reference voltage, thereby generating the modulation index for each cell. The main drawbacks of this strategy are the inherent distortion produced in the cluster output voltages and that its performance depends on the gain of the proportional controller. In [18], a design criterion to confine the steady-state error for the capacitor voltages is introduced.

On the other hand, in [9, 19], a priority list of cells is used for balancing the capacitor voltages and the output voltage is built by modulating only one cell per period and keeping the rest of the cells either on or off during the full switching cycle. For properly balancing the capacitor voltages, the assignment of cells is based on the sorted capacitor voltages and the charging/discharging cluster state. This method does not require tuning control parameters; hence, it is decoupled from the inner current control loop. Nevertheless, this approach could increase the average switching frequency of the semiconductor devices [20]. In addition, the sorting algorithm could lead to a huge level of arithmetic complexity, limiting the application of this strategy to converters with a reduced number of cells. In this regard, a partial sorting based on maximum and minimum capacitor voltage's index is proposed for several control approaches applied to the MMCs [13, 14].

This paper presents a novel CVB strategy based on continuous control set model predictive control (CCS-MPC). The proposed capacitor voltage balancing method computes an optimal modulation index for each cell using the analytical solution derived from the dual formulation of the CCS-MPC. This solution does not introduce an error into the output voltage, and it presents a structure that allows using it with PS-PWM. Additionally, this paper proposes a slight modification of the method introduced in [11] [12] with the purpose of eliminating the output voltage error produced by the original algorithm.

Experimental results are obtained for both CVB strategies analyzed in this paper from a single-phase arm converter with nine cells. A comparison between them is performed under both stationary and transient operating conditions considering also different modulation indexes.

II. Capacitor Voltage Balancing Strategies

The aims of a CVB method in a MMC topology are to simultaneously control the mean value of each capacitor voltage and modulate the required output voltage with a given circulating current i_o. The typical structure of the cluster is depicted in Fig. 1(b), where n full-bridges are connected in series. The series connection of the cluster with an inductor L_B defines the arm (or branch).

For modeling, let us considers that the j-th capacitor has a capacity of C_j, and a voltage of value u_{Cj}. On the AC side of each cell, the voltage generated is v_{oj}, which instantaneously depends on the state of the switches $s_j \in \{-1, 0, 1\}$ and capacitor voltage u_{Cj}. The set of all cells will be denoted as $\mathcal{K} = \{1, \ldots, n\}$, the desired output voltage to be modulated is v_o^*, and the reference voltage for each capacitor is u_{Cj}^*. Furthermore, a small switching cycle T_s will be assumed.

Thereby, for each cluster, the modulation problem can be considered as an optimal control problem defined as:

$$\textbf{(P1)} \qquad \min_{U_{Cj}, m_j} \quad \sum_{j\in\mathcal{K}} \left(u_{Cj}^* - U_{Cj}\right)^2 \tag{1a}$$

$$\text{s.t.} \qquad C_j \frac{dU_{Cj}}{dt} = i_o m_j \qquad \forall j \in \mathcal{K} \tag{1b}$$

$$\sum_{j\in\mathcal{K}} u_{Cj} m_j = v_o^* \tag{1c}$$

$$m_j \in [-1, 1] \qquad \forall j \in \mathcal{K} \tag{1d}$$

In this formulation, continuous variables integrated within a switching cycle have been denoted as $X = \frac{1}{T_s}\int_0^{T_s} x(t)\,dt$, and integrals over products between continuous and switching states are approximated using first order Taylor series around the point $(x, s) = (x(0), 0)$ as:

$$\frac{1}{T_s}\int_0^{T_s} x(t)\, s(t) dt \simeq x(0)\, m.$$

where m is the modulation index, which is defined within the interval $m \in [-1, 1]$ for full-bridge cells.

In (**P1**), the constraint (1c) means that the desired output voltage v_o^* has to be generated by properly selecting the modulation index for each cell m_k. It follows that these variables will be the control actions for solving the underlying optimization problem.

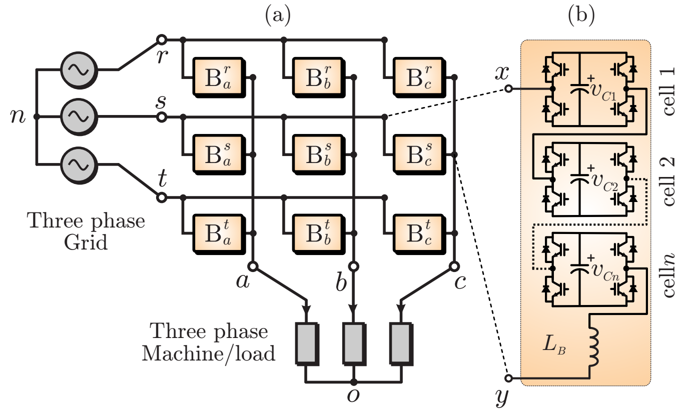

Fig. 1. (a) Modular Multilevel Matrix Converter (M3C): (a) topology; (b) arm composed by n cells and an inductive filter.

Using forward Euler method to discretize (1b), variables U_{Cj} can be eliminated from the problem (**P1**), then:

$$\textbf{(P2)} \qquad \min_{m_j} \quad \sum_{j\in\mathcal{K}} \left(u_{Cj}^k - U_C^* + \Delta u_{\max}^k m_j^k\right)^2 \tag{2a}$$

$$\text{s.t.} \qquad \sum_{k\in\mathcal{K}} u_{Cj}^k m_j^k = v_o^* \tag{2b}$$

$$m_j^k \in [-1, 1] \qquad \forall j \in \mathcal{K} \tag{2c}$$

where

$$\Delta u_{\max}^k = \frac{T_s}{C} i_o^k \tag{3}$$

is the maximum increment/decrement of the capacitor voltage when full modulation index is applied to the cell; thus, the balancing capability is affected by the magnitude of the arm current at instant t_k.

It is worth noting here that the reformulated optimization problem (**P2**) corresponds to a continuous control set model predictive control (CCS-MPC) [21] since the future value of the capacitor voltages u_{Cj}^{k+1} is used in the objective function as a function of the modulation index m_j^k and the sampled capacitor voltage u_{Cj}^k at instant t_k.

A. *Proposed CVB strategy (Method-I)*

In the following, the CVB strategy to solve the optimization problem defined by (**P2**) is derived. The proposed approach relaxes certain constraints of this problem preserving its original objective function. In this regard, the upper and lower bounds for the modulation index [see (1d)] are ignored.

Considering the above, the following dual formulation is derived from **(P2)**,

$$\textbf{(P2d)} \qquad \max_{\lambda} \min_{|m_j|\le 1} \quad \sum_{j\in\mathcal{K}} \left(u_{Cj}^k - U_C^* + \Delta u_{\max}^k m_j^k\right)^2 + \lambda\Big(v_o^* - \sum_{j\in\mathcal{K}} u_{Cj}^k m_j^k\Big) \tag{4}$$

For the sake of simplicity, in the following, the superscript k, which is denoting the sampling instant, is omitted.

Since the inner problem of **(P2d)** is the sum of one–dimensional positive definite quadratic problems, its relaxed solution, when bounds over modulation index m_j are not considered, is given by:

$$m_j(\lambda) = \frac{u_{Cj}}{2\Delta u_{\max}^2}\lambda + \frac{U_C^* - u_{Cj}}{\Delta u_{\max}} \quad (5)$$

Replacing (5) in the constraint (2b), and by solving for the Lagrange multiplier, we have:

$$\lambda = \frac{2\Delta u_{\max}^2}{\sum_{j\in\mathcal{K}} u_{Cj}^2}\left(v_o^* - \frac{1}{\Delta u_{\max}}\Big(\sum_{j\in\mathcal{K}} U_C^* u_{Cj} - \sum_{j\in\mathcal{K}} u_{Cj}^2\Big)\right) \quad (6)$$

Therefore, the unconstrained optimum of (**P2**) is finally obtained and it can be computed according to:

$$m_j = \frac{v_o^*}{U_C^*}\Omega_j + \frac{1}{\Delta u_{\max}}\left(U_C^* - u_{Cj}\sum_{i\in\mathcal{K}}\Omega_i\right), \quad (7)$$

where

$$\Omega_j = \frac{u_{Cj}U_C^*}{\sum_{i\in\mathcal{K}} u_{Ci}^2}, \quad (8)$$

is a dimensionless parameter that contains information of each cell voltage weighted somehow by the overall cluster energy.

As illustrated in (7), the relaxed solution of the optimal control problem (P2) has two components: the first one proportional to the commanded output voltage v_o^* weighted by Ω_j, meanwhile the second one depends on the balancing capability of the cluster and it is proportional to an equivalent capacitor voltage error, which measures the difference between the capacitor voltage reference U_C^* and the cell voltage u_{Cj} weighted by the sum of the parameters Ω_j over all cells. It follows that the proposed CVB strategy has a global view of the cluster which allows it balancing the capacitor voltages.

On the other hand, the structure of (7) does not allow to define a proper modulation scheme at a glance. However, assuming that all capacitor voltages are well regulated with instantaneous values close to U_C^*, which is the desired steady-state operation, then the optimal solution (7) can be approximated as

$$m_j \simeq m_0 + \left(\frac{1}{\Delta u_{\max}} - \frac{m_0}{U_C^*}\right)\left(U_C^* - u_{Cj}\right) \quad (9)$$

being

$$m_0 = \frac{v_o^*}{\sum_{i\in\mathcal{K}} u_{Ci}}. \quad (10)$$

Therefore, the optimal solution requires injecting a common modulation index to all cells (m_0) with a slight correction proportional to the capacitor voltage error. Taking into account this feature of the solution under steady-state conditions, where an almost even modulation index distribution among cells is achieved, in this work, the PS-PWM strategy is proposed to synthesize the output voltage when the modulation indexes are computed according to (7) In consequence, the switching frequency harmonic cancellation, due to the carrier signals phase-shifted, is accomplished and, the total harmonic distortion of the output voltage can be minimized [15].

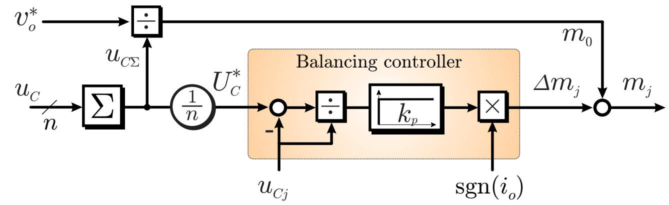

Fig. 2. Signal flow of the modified CVB method introduced in [11, 12].

Unlike the local balancing capacitor voltage control introduced in [7] [11] [12], one of the main advantages of the optimal solution (7) is that it always satisfies the constraint (1c). Therefore, no distortion at the synthesized voltage would be introduced by the converter, and the output cluster voltage averaged over a switching cycle will be, ideally, equal to the reference voltage v_o^*.

B. Modified CVB strategy based on P-controllers (Method-II).

In this section, a slight modification of the local balancing strategy introduced in [12] is addressed to cancel the distortion in the output voltage produced by the original algorithm. This balancing method adds a compensating signal to each cell, which is a result of the comparison between related cell's capacitor voltage and its reference value.

Due to the integral effect of the plant (power/voltage cell-model [2] [4]), a proportional controller is used. Thereby, the additional signal introduced by this strategy depends on the current direction and the capacitor voltage error according to

$$\Delta m_j = k_p \mathrm{sgn}(i_o)(U_C^* - u_{Cj}) \quad (11)$$

being k_p>0, a tuning parameter. It follow that this additional term modifies the modulation index previously calculated by the control algorithm, leading to the following averaged output distortion voltage:

$$\Delta V_o = \sum_{j\in\mathcal{K}} \Delta m_j u_{Cj}, \quad (12)$$

which negatively affects the performance of the modulator and the overall converter.

However, by normalizing each capacitor voltage error by the voltage in each cell, u_{Cj}, the voltage distortion (12) becomes

$$\Delta V_o = \sum_{k\in\mathcal{K}} \Delta m_j = k_p \mathrm{sgn}(i_o)\left(nU_C^* - \sum_{j\in\mathcal{K}} u_{Cj}\right). \quad (13)$$

Then, ΔV_o can be overridden as long as the reference U_C^* is set as the average value of the capacitor voltages:

$$U_C^* = \frac{1}{n}\sum_{j\in\mathcal{K}} u_{Cj} = \frac{1}{n}u_{C\Sigma}. \quad (14)$$

In consequence, if the modulation index is computed as

$$m_j = m_0 + k_p\,\mathrm{sgn}(i_o)\frac{1}{u_{Cj}}\left(\frac{u_\Sigma}{n} - u_{Cj}\right), \quad (15)$$

it is straightforward to demonstrate, by replacing (15) into (1c), that the generated output voltage will be the desired one.

It follows that no voltage distortion will be injected by the modified local balancing methodology. The resulting signal flow is illustrated in Fig. 2.

Like the proposed CVB strategy, this method uses the PS-PWM to generate the firing pulses for the semiconductors since it introduces a common modulating signal to all cells.

III. Conditions and control system for testing the CVB strategies

For the MMC topologies, the conventional methodology to perform an specific performance criterion versus variation of the modulation index can not be directly carried out since the cells are composed of floating capacitors and a current flowing between all cells is required to balance their energy [2]. Besides, depending on the operating point, oscillations of different amplitude and frequency can be produced in capacitor voltages.

To overcome this drawback, the magnitude of the capacitor voltage ripple is keep fixed over the whole modulation range to be tested. Therefore, by respecting aforementioned condition, the test could be performed in only one cluster, since each CVB scheme will be applied to the converter considering the same generalized operating condition. As shown in Fig. 1(b), the point in which the cells will be operating depends on the amplitude and frequency of both the voltage between the input terminals of a cluster, v_{xy}, and the current flowing between them i_o. Taking into account that an arbitrary voltage source provides the voltage v_{xy}, a current control loop has to be implemented to fulfill the second operating condition.

Aiming to model the amplitude of the capacitor voltage ripple as a function of the modulation index, steady state operation is assumed. Under this condition, the amplitude, frequency, and phase-angle of the input voltage are $V_{\rm s}$, $\omega_{\rm s}$, and $\theta_{\rm s}$, respectively. In addition, the arm current can be conveniently decomposed in two orthogonal terms as

$$i_{\rm o} = I_{\rm d}\cos\theta_{\rm s} - I_{\rm q}\sin\theta_{\rm s}. \tag{16}$$

On the other hand, by assuming that the capacitors voltages are well regulated with instantaneous value close to U_C^*, the following small signal model, that relates the sum of the capacitors voltages with the cluster instantaneous power p_o, is derived [2] [4]:

$$CnU_C^*\frac{d\Delta u_C}{dt} = p_{\rm o} - p_{\rm loss} \tag{17}$$

being $p_{\rm loss}$, the total power losses of the cluster. Then, by replacing (16) in (17), the latter equation becomes

$$CnU_C^*\frac{d\Delta u_C}{dt} = \frac{V_{\rm o}I_{\rm d}}{2} - p_{\rm loss} + \frac{V_{\rm o}}{2}(I_{\rm d}\cos 2\theta_s - I_{\rm q}\sin 2\theta_s) \tag{18}$$

where $V_{\rm o}$ is the amplitude of the cluster output voltage.

Consequently, an average control scheme for the capacitor voltages with a nested current loop can be established. In this regard, $I_{\rm d}$ regulates the active power injected to compensate the cluster losses allowing to control the available cluster voltage $v_{C\Sigma}$ to its desired value. Likewise, $I_{\rm q}$ generates an oscillatory instantaneous power fluctuating at $2\omega_{\rm s}$, which inherently produces a voltage ripple of the same frequency. Indeed, if the cluster power losses are assumed negligible, the amplitude of the capacitor voltage ripple in steady state can be approximated by

$$|\Delta u_C| \approx \frac{(V_{\rm s} - \omega_{\rm s}L_{\rm B}I_{\rm q})I_{\rm q}}{4\omega_{\rm s}CnU_C^*} = \frac{m_0 I_{\rm q}}{4\omega_{\rm s}C}. \tag{19}$$

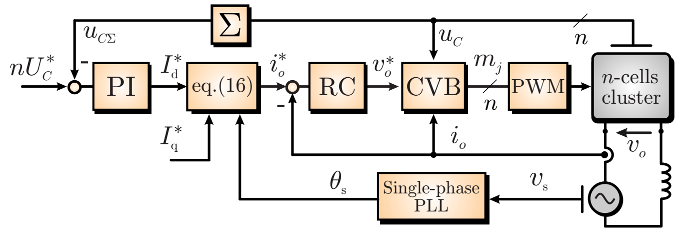

Fig. 3. General control scheme for testing the CVB strategies.

In consequence, to keep constant the magnitude of Δu_C against changes in the modulation index m_0, it is indispensable to vary both $V_{\rm s}$ and $I_{\rm q}$ in order to satisfy (19).

Fig. 3 shows the resulting control system for testing the modulation schemes analysed in this paper. It can be seen that the inner current loop is based on a resonant controller (RC), whose reference signal is obtained from (16) by using a single-phase PLL [22].

IV. Experimental Results

To validate and compare the balancing schemes introduced in section II, an experimental system is set up with nine H-bridges cells. The control algorithm illustrated in Fig 3 is implemented in a TMS320C6713 DSP board coupled with an Xilinx FPGA model XC6SLX16-2FTG256.

The prototype parameters are C=1800μF, $L_{\rm B}$=7.5mH, and the dead-time is set to 2μs. The MOSFET used in each cell is the IRFI4321PBF model, and the input voltage source is provided by a programmable AC source AMETEK CSW5550.

The CVB strategies presented in section II were tested, and their performances were evaluated for a nine-cells cluster configuration under stationary and transient operating conditions.

A. Steady-State operation

The experimental results of the proposed CVB strategy for three different modulation indexes with an available cluster voltage $nU_C^* = 300$V are depicted in Fig. 4. Due to oscilloscope available number of channels, only three capacitor voltage waveforms are registered, and their average values can be directly read from the right-hand menu. As shown in Fig. 4, despite of changing the modulation index, the capacitor voltages are well regulated around 33V with 7.25V of ripple in all cases, which experimentally validates the methodology exposed in section III to keep constant the magnitude of the capacitor voltage ripple independently of the duty cycle.

On the other hand, from the operation with $m = 0.9$ shown in Fig. 4(c), it is seen that 19 levels are generated in the output voltage (maximum available), which are reduced to 9 when the modulation index is changed to $m = 0.4$ [see Fig. 4(a)]. This

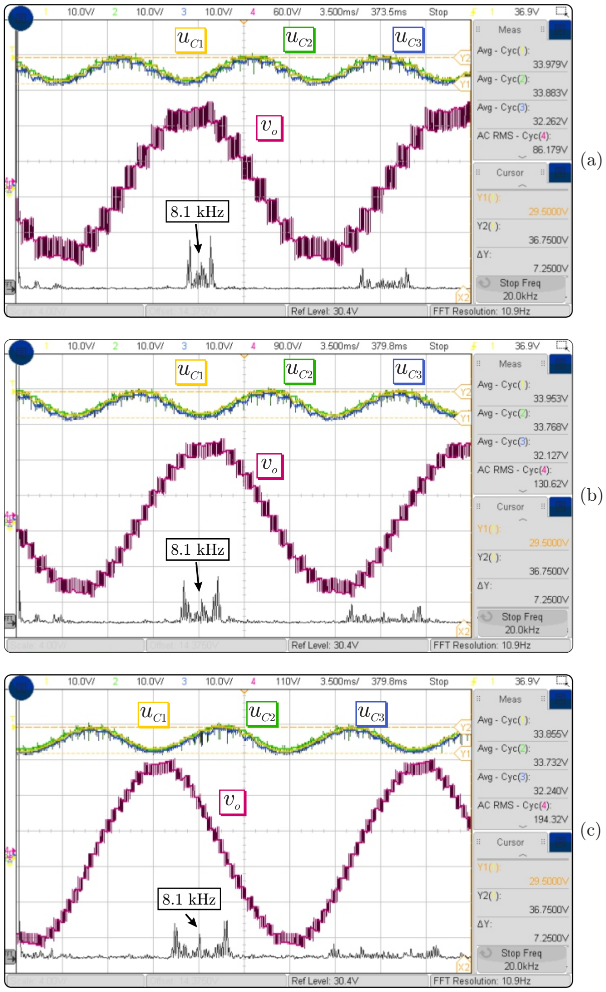

Fig. 4. Experimental waveforms of the proposed CVB strategy for 1000 VAr considering several modulation indexes with fixed capacitor voltage ripple criterion (19): (a) $m = 0.4$; (b) $m = 0.6$; and (c) $m = 0.9$.

behavior is typical of PS-PWM strategy. Besides, as shown the right-hand menu, the AC-RMS values of the output voltage vary in the same proportion as the modulation indexes do.

The output voltage frequency spectrum is directly obtained from the oscilloscope considering 2kHz/division. As depicted in Fig. 4, the first dominant high frequency harmonics are centered around 8.1 kHz for all cases, being consistent with the number of cells and the set carrier frequency (450 Hz). However, the components at 0.9 and 1.8 kHz in the harmonic spectrum are not completely canceled by the PS-PWM strategy since all modulation indexes are not identical, as it can be seen in the proposed analytical solution given in (7).

On the other hand, Fig. 5 shows the experimental waveforms obtained with both CVB strategies analyzed in this paper considering a modulation index m=0.8. In this case, the reactive power is 1500 VAr, which leads to 9.6 V the capacitor voltage ripple. Comparing both responses, no significant differences can be established; however, it is worth to emphasize the slight contrast between the harmonic spectra obtained with both strategies. This discrepancy is due to the way as

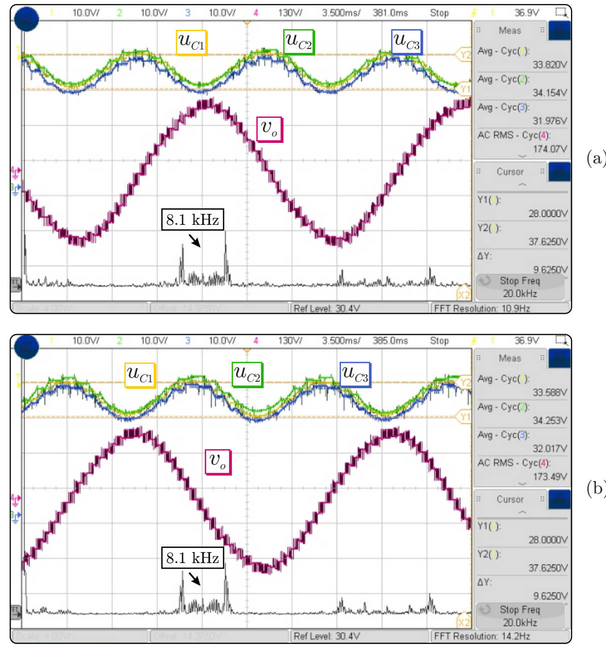

Fig. 5. Waveform comparison between both CVB strategies presented in this paper for 1500 VAr and $m = 0.8$ with fixed capacitor voltage ripple criterion (19): (a) method I; (b) method II.

the modulation indexes are computed since both balancing strategies are using the same PS-PWM configuration.

B. OFF-ON test

This test consists on disabling the balancing control scheme and then activate it when any of the capacitor voltages reaches a threshold of $\pm 50\%$ of their reference value. An overview of the resulting capacitor voltage waveforms for both strategies is shown in Fig. 6. As depicted in the graphics (b) and (c), the performance of the Method-II is evaluated for two different P-controller tuning. Comparing these transient responses, the experiment demonstrates that the proposed CVB strategy has a faster balancing response than Method-II in both cases.

Finally, the Fig. 7 shows the output voltage and current waveforms obtained with the proposed CVB strategy during the same OFF-ON test depicted in Fig. 6(a) for the capacitor voltages. As can be seen, at instant t=0, the CBV scheme is enabled, and the required balance condition is achieved in a short time, moreover, the output voltage waveform reach its regular shape in a quarter of its fundamental period. Therefore, the proposed CVB scheme allows a better output voltage waveform during transients.

V. Conclusions

This paper presents a novel control method to balance the capacitor voltages on modular multilevel converters. This strategy computes an optimal modulation index for each cell using the analytical solution of an optimal control problem. Due to its structure, the Capacitor Voltage Balancing (CVB) strategy is integrated to phase-shifted PWM scheme in order

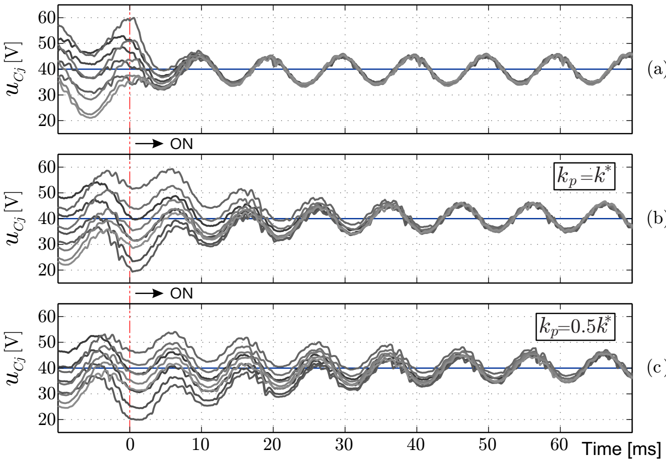

Fig. 6. Capacitor voltage waveforms for OFF-ON testing with m=0.7, S=2000 VAr and $v_{C\Sigma}$=360V: (a) Proposed strategy; (b) Method-II; (c) Method-II with half of the gain k^*.

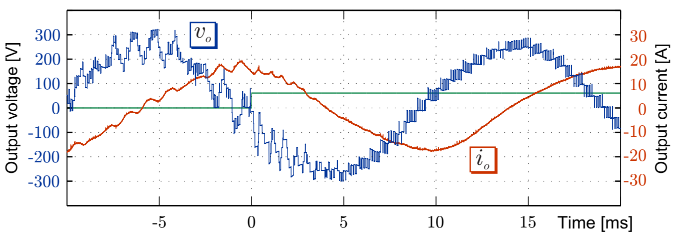

Fig. 7. Output voltage and current waveforms obtained with the proposed CVB strategy during the OFF-ON test.

to minimize the total harmonic distortion of the synthesized output voltage.

Comparing the performance of the proposed CVB method with the modified local balancing strategy, it was verified that there are no significant differences under steady-state operating conditions. However, during transients, the proposed method achieves the balancing of the capacitor voltages faster than the modified original strategy.

Acknowledgment

This work was supported by CONICYT-FONDECYT through research grant Project 1140337. Additionally, the support of the CONICYT Basal Project FB0008, "Advanced Center for Electrical and Electronic Engineering" is kindly acknowledged.

References

[1] S. Kouro, M. Malinowski, K. Gopakumar, J. Pou, L. G. Franquelo, B. Wu, J. Rodriguez, M. A. Perez, and J. I. Leon, "Recent advances and industrial applications of multilevel converters," *IEEE Trans. Ind. Electron.*, vol. 57, pp. 2553–2580, Aug 2010.

[2] M. A. Perez, S. Bernet, J. Rodriguez, S. Kouro, and R. Lizana, "Circuit topologies, modeling, control schemes, and applications of modular multilevel converters," *IEEE Trans. Power Electron.*, vol. 30, pp. 4–17, Jan 2015.

[3] H. Akagi, "Classification, terminology, and application of the modular multilevel cascade converter (mmcc)," *IEEE Trans. Power Electron.*, vol. 26, pp. 3119–3130, Nov 2011.

[4] M. Espinoza, R. Cárdenas, M. Díaz, and J. C. Clare, "An enhanced *dq*-based vector control system for modular multilevel converters feeding variable-speed drives," *IEEE Trans. Ind. Electron.*, vol. 64, pp. 2620–2630, April 2017.

[5] S. Shao, A. J. Watson, J. C. Clare, and P. W. Wheeler, "Robustness analysis and experimental validation of a fault detection and isolation method for the modular multilevel converter," *IEEE Trans. Power Electron.*, vol. 31, pp. 3794–3805, May 2016.

[6] D. Braeckle, F. Kammerer, M. Schnarrenberger, M. Hiller, and M. Braun, "A modular multilevel matrix converter for high speed drive applications," in *PCIM Europe 2016; International Exhibition and Conference for Power Electronics, Intelligent Motion, Renewable Energy and Energy Management*, pp. 1–8, May 2016.

[7] M. Díaz, M. Espinoza, A. Mora, R. Cárdenas, and P. Wheeler, "The application of the modular multilevel matrix converter in high-power wind turbines," in *18th European Conference on Power Electronics and Applications (EPE'16 ECCE Europe)*, pp. 1–11, Sept 2016.

[8] Y. Okazaki, W. Kawamura, M. Hagiwara, H. Akagi, T. Ishida, M. Tsukakoshi, and R. Nakamura, "Experimental comparisons between modular multilevel dscc inverters and tsbc converters for medium-voltage motor drives," *IEEE Trans. Power Electron.*, vol. 32, pp. 1805–1817, March 2017.

[9] F. Kammerer, J. Kolb, and M. Braun, "A novel cascaded vector control scheme for the modular multilevel matrix converter," in *IECON 2011 - 37th Annual Conference of the IEEE Industrial Electronics Society*, pp. 1097–1102, Nov 2011.

[10] F. Kammerer, M. Gommeringer, J. Kolb, and M. Braun, "Energy balancing of the modular multilevel matrix converter based on a new transformed arm power analysis," in *2014 16th European Conference on Power Electronics and Applications*, pp. 1–10, Aug 2014.

[11] W. Kawamura, M. Hagiwara, and H. Akagi, "Control and experiment of a modular multilevel cascade converter based on triple-star bridge cells," *IEEE Trans. Ind. Appl.*, vol. 50, pp. 3536–3548, Sept 2014.

[12] M. Hagiwara and H. Akagi, "Control and experiment of pulsewidth-modulated modular multilevel converters," *IEEE Trans. Power Electron.*, vol. 24, pp. 1737–1746, July 2009.

[13] J. Mei, K. Shen, B. Xiao, L. M. Tolbert, and J. Zheng, "A new selective loop bias mapping phase disposition pwm with dynamic voltage balance capability for modular multilevel converter," *IEEE Trans. Ind. Electron.*, vol. 61, pp. 798–807, Feb 2014.

[14] W. Li, L. A. Grégoire, and J. Bélanger, "A modular multilevel converter pulse generation and capacitor voltage balance method optimized for fpga implementation," *IEEE Trans. Ind. Electron.*, vol. 62, pp. 2859–2867, May 2015.

[15] B. Wu, *High-Power Converters and AC Drives*. Wiley-IEEE Press, 2006.

[16] J. I. Y. Ota, Y. Shibano, N. Niimura, and H. Akagi, "A phase-shifted-pwm d-statcom using a modular multilevel cascade converter (ssbc) – part i: Modeling, analysis, and design of current control," *IEEE Trans. Ind. Appl.*, vol. 51, pp. 279–288, Jan 2015.

[17] B. P. McGrath, T. Meynard, G. Gateau, and D. G. Holmes, "Optimal modulation of flying capacitor and stacked multicell converters using a state machine decoder," *IEEE Trans. Power Electron.*, vol. 22, pp. 508–516, March 2007.

[18] Y. Okazaki, H. Matsui, M. M. Muhoro, M. Hagiwara, and H. Akagi, "Capacitor-voltage balancing for a modular multilevel dscc inverter driving a medium-voltage synchronous motor," *IEEE Trans. Ind. Appl.*, vol. 52, pp. 4074–4083, Sept 2016.

[19] R. E. Betz, T. J. Summers, and G. Mirzaeva, "Dead-time compensation for multilevel cascaded h-bridge converters with novel voltage balancing," in *2009 13th European Conference on Power Electronics and Applications*, pp. 1–10, Sept 2009.

[20] J. Qin and M. Saeedifard, "Reduced switching-frequency voltage-balancing strategies for modular multilevel hvdc converters," *IEEE Trans. Power Del.*, vol. 28, pp. 2403–2410, Oct 2013.

[21] D. E. Quevedo, R. P. Aguilera, and T. Geyer, *Predictive Control in Power Electronics and Drives: Basic Concepts, Theory, and Methods*, pp. 181–226. Cham: Springer International Publishing, 2014.

[22] R. Teodorescu, M. Liserre, and P. Rodriguez, *Grid converters for photovoltaic and wind power systems*. Wiley-IEEE Press, 2011.